

## An investigational study on Synthesis and energy conversion on Tungsten Oxide Nano flakes

<sup>1</sup>B.Narasimha Rao, <sup>2</sup>S.Rama Krishna, <sup>3</sup>N Vijaya Lakshmi

<sup>1,2,3</sup>Assistant Professor, Dept. of BS &H, Newton's Institute of Engineering, Macherla, Andhra Pradesh, India.

### Abstract

We used the hydrothermal approach to create nano-sized tungsten oxide (WO<sub>3</sub>) flakes. Utilizing X-ray diffraction (XRD), scanning electron microscopy (SEM), and high-resolution X-ray photoelectron spectroscopy methods, the structural characteristics of the as produced WO<sub>3</sub> nanoflakes were examined (XPS). Furthermore, the basic vibration modes of WO<sub>3</sub> flakes were further shown by Raman spectra. The distinctively nano structured WO<sub>3</sub> has demonstrated a fresh option for energy storage and energy conversion materials.

**Keywords:** WO<sub>3</sub>, nano flakes, XRD, XPS and Raman spectroscopy

### Introduction

Ozone-based semiconductor materials [1-3] have drawn a lot of interest in recent years due to their usefulness in solving energy and environmental problems [4-7]. Due to its consistent physicochemical characteristics, resistance to photocorrosion in aqueous solution, and apparent light sensitive qualities, tungsten oxide (WO<sub>3</sub>) is one of the most promising materials among them [3, 8]. Though, due to the high rate of electron-hole recombination, WO<sub>3</sub> nanoparticles are often ineffective catalysts and photocatalysts [8]. Numerous initiatives have been made to address this limitation of surface regulations, including appropriate textural design [9], the construction of certain morphologies with high-surface-energy facets [10], or the development of heterojunctions [11]. Among these, the modification of structure has attracted a lot of attention due to its facile effectiveness in improving the separation between electron hole pairs and thus improves the performance for energy conversion and storage applications. Many important findings have been reported on the structure tuning during the past few years [4, 12-14]. It was demonstrated that the structure of WO<sub>3</sub> could alter alone and/or with various semiconductors, such as the typical photocatalysts, including UV-light driven TiO<sub>2</sub> [15], the visible light driven BiVO<sub>4</sub> [16], g-C<sub>3</sub>N<sub>4</sub> [17], Ag<sub>3</sub>PO<sub>4</sub> [18], photocatalysts and so on. Although structure modifications on photocatalysts is an effective method for enhancing the photocatalytic activity [19], more studies have been done to improve the activity of WO<sub>3</sub> itself by simple structure modifications and has been demonstrated to be efficient in the electron-hole separation [20-22]. Besides, the structure modified WO<sub>3</sub> can be more feasible and practical [23]. Hence, it is essential to examine the structural transformation in WO<sub>3</sub> for an efficient device fabrication. Among all the crystalline phases of WO<sub>3</sub>, monoclinic (m-WO<sub>3</sub>) and hexagonal (h-WO<sub>3</sub>) are typically used as photocatalyst in water splitting, and hexagonal (h-WO<sub>3</sub>) endures a phase transition to monoclinic-WO<sub>3</sub> phase through calcination [24]. In this work, an interesting surface morphology of flakes structures was obtained for WO<sub>3</sub>, i.e. monoclinic phase (m-WO<sub>3</sub>). Further, XRD, XPS and Raman spectroscopies were conducted to confirm the monoclinic phase of WO<sub>3</sub>. It is found that the contents of WO<sub>3</sub> can be precisely adjusted by the calcination temperature. An in-depth understanding of nanostructure-related disputes may be a great support in the design and fabrication of efficient semiconductor based materials.

### Materials and Methods

#### Materials synthesis

The precursor was prepared by dissolving 1.0 g Sodium Tungstate dihydrate (Na<sub>2</sub>WO<sub>4</sub>·2H<sub>2</sub>O) as tungsten (W) source in 80 ml of 6 M Hydrochloric acid (HCl) under 1 h stirring to form H<sub>2</sub>WO<sub>4</sub> solution. Then 30 ml of 2 g Ammonium Nitrate (NH<sub>4</sub>NO<sub>3</sub>) solution for controlling monoclinic structure was mixed in the solution for the

synthesis of  $\text{WO}_3$  flakes. The precursors solution were transferred into 100 ml Teflon-lined stainless steel autoclave, which was processed at  $200^\circ\text{C}$  for 20 h. At the execution of the process, the resultant precipitates of light-yellow (flakes) were separated by purifying, washed with distilled water to remove the remaining ions and ethanol to facilitate the evaporation of water, and finally dried at  $180^\circ\text{C}$  in air for 12 h.

## 2.2 Materials characterization

The crystalline phases of the prepared samples were examined using X-ray diffraction (XRD) analysis (Bruker AXS D8, Bruker, Germany). The surface morphology of the samples was examined by field-emission scanning electron microscopy (FE-SEM; JSM 6500F). The chemical composition and elements present in samples and their corresponding valence states in samples were determined by X-ray photoelectron spectroscopy (XPS). The measurements were acquired by an ESCALab220i-XL electron spectrometer (Thermo Fisher Scientific Company, USA). The vibrational, rotational and other low-frequency modes in the sample were analyzed by Raman spectroscopy (Thermo Scientific DXR).

## Results and Discussions

XRD pattern of synthesized  $\text{WO}_3$  by the hydrothermal process is shown in Fig. 1. All X-ray diffraction peaks are consistent with those predictable for monoclinic  $\text{WO}_3$  phase (m- $\text{WO}_3$ ), matching to the JCPDS No. 83-0950 as normal.[24] No any other impurities were perceived, offering that the final product is pure phase. Peak intensities are high and sharp, representing the very good crystalline nature of the final  $\text{WO}_3$  product. It is worth to note that the strong diffraction peak of the (0 0 2) plane is higher than those of other diffraction planes, revealing the m- $\text{WO}_3$  structure with vastly anisotropic growth in the c-axis. The average size of the ordered  $\text{V}_2\text{O}_5$  nanoparticles has been assessed from Debye- Scherrer formula [25-27] according to equation the following:  
 $D = 0.89 \lambda / \beta \cos\theta$  where, 0.89 is the shape factor,  $\lambda$  is the x-ray wavelength,  $\beta$  is the line widening at half the maximum intensity (FWHM) in radians, and  $\theta$  is the Bragg angle. The average size of  $\text{WO}_3$  nanoflakes was around  $\sim 29$  nm from this Debye-Scherrer equation.

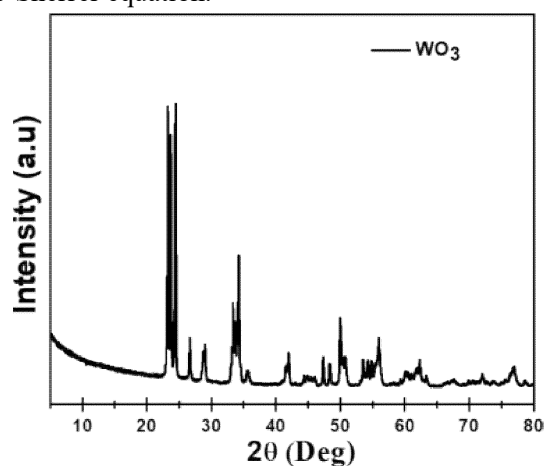


Fig. 1 XRD pattern of  $\text{WO}_3$

Surface morphologies of the prepared sample were investigated by scanning electron microscope (SEM). SEM image of m- $\text{WO}_3$  synthesized (Fig. 2) shows the flakes over the range of  $0.50\text{--}1.00$   $\mu\text{m}$  wide and  $0.30\text{--}0.50$  m thick.

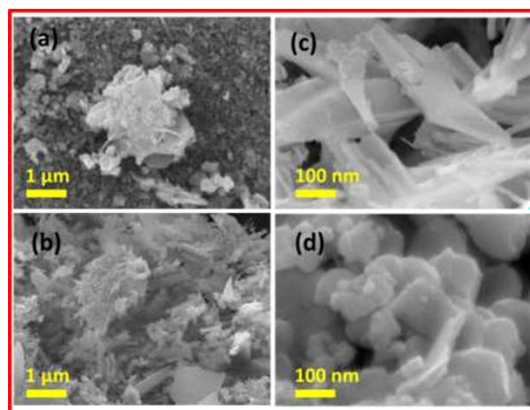


Fig. 2. FE-SEM images of WO<sub>3</sub> flakes

The low and high magnifications clearly indicated as the m-WO<sub>3</sub> flakes structure and no exposure of other morphologies. Formation mechanisms of m-WO<sub>3</sub> nanoplates and nanorods are able to be described as follows [28-30].



By dissolving sodium tungstate dihydrate, the colorless solution made. Then this colorless solution converted into the yellow one upon addition of HCl solution, thus show the possible formation of tungstic acid solution. Under hydrothermal action, the tungstic acid in the existence of NH<sub>4</sub>NO<sub>3</sub> decomposed into flakes shaped m-WO<sub>3</sub>. Under hydrothermal system, WO<sub>3</sub> nuclei quickly made from the precursor; then these nuclei served as seeds, produced due to self-assembled method and developed into m-WO<sub>3</sub> flakes.

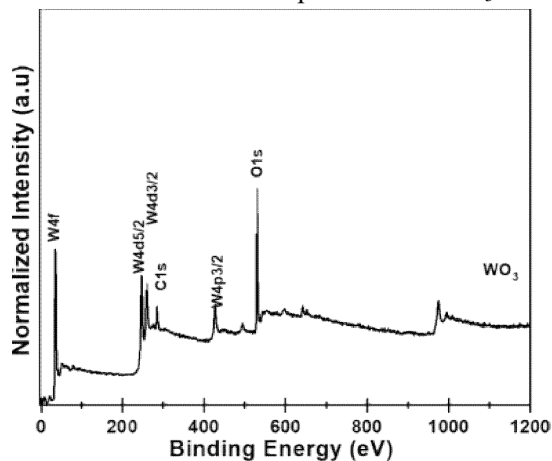
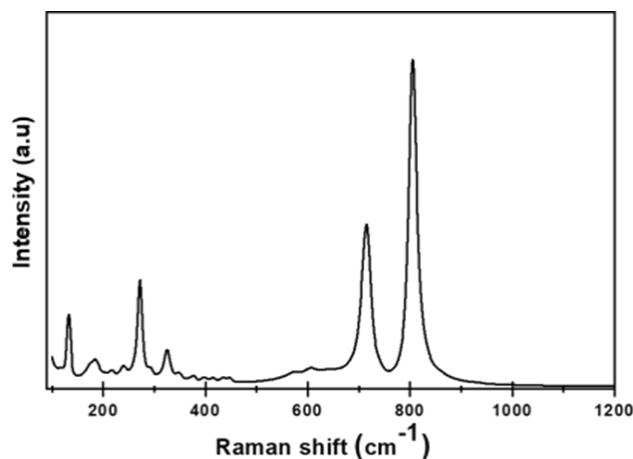


Fig. 3 XPS spectra of WO<sub>3</sub>



**Fig. 4** Raman spectra of  $\text{WO}_3$

As shown in Fig. 3, two sharp peaks with binding energies at 35.63 and 37.71 eV can be observed, which are related with the characteristic  $W4f_{7/2}$  and  $4f_{5/2}$  peaks of the  $W^{6+}$  species, besides they indicate the co-existence of  $W^{5+}$  ions with oxygen (O) vacancies, the elemental composition of W is about 35 %. [31, 32]. That fact is also reflected by characteristic O 1s photoemission lines located at 531.6 eV. Fig. 4 presents the Raman spectra of the prepared catalysts, where the peaks at  $273\text{ cm}^{-1}$  and  $326\text{ cm}^{-1}$  are due to the O–W–O bending vibration, and the peaks at  $716\text{ cm}^{-1}$  and  $807\text{ cm}^{-1}$  are ascribed to the O–W–O stretching vibration.[33, 34] From these results, it may be concluded that  $\text{WO}_3$  is perfectly produced with flakes structure. This unusual property is highly preferred and can be deliberated as an encouraging strategy to improve the electro catalytic and photo catalytic activity of tungsten oxide based systems.

## Conclusions

The hydrothermal technique was effective in producing monoclinic  $\text{WO}_3$  nano flakes.  $\text{WO}_3$ 's phase was managed during the synthesis. XRD, XPS, and Raman spectroscopy all verified that the m- $\text{WO}_3$  nano plates were in their pure phase. The distinctively nano structured m- $\text{WO}_3$  has demonstrated a fresh option for energy storage and energy conversion materials.

## References

- [1] Y. Abozeid, G.R. Williams, Wiley Interdisciplinary Reviews: Nanomedicine and Nanobiotechnology, 12 (2020) e1592.
- [2] S. Chandrasekaran, E.J. Kim, J.S. Chung, C.R. Bowen, B. Rajagopalan, V. Adamaki, R. Misra, S.H. Hur, Journal of Materials Chemistry A, 4 (2016) 13271-13279.
- [3] S. Chandrasekaran, P. Zhang, F. Peng, C. Bowen, J. Huo, L. Deng, Journal of materials chemistry A, 7 (2019) 6161-6172.
- [4] S. Chandrasekaran, L. Yao, L. Deng, C. Bowen, Y. Zhang, S. Chen, Z. Lin, F. Peng, P. Zhang, Chemical Society Reviews, 48 (2019) 4178-4280.
- [5] S. Chandrasekaran, J.S. Chung, E.J. Kim, S.H. Hur, J Electrochem Sci Technol, 7(2016) 1-12.
- [6] M.T. Greiner, M.G. Helander, W.-M. Tang, Z.-B. Wang, J. Qiu, Z.-H. Lu, Nature materials, 11 (2012) 76.
- [7] S. Chandrasekaran, Solar energy materials and solar cells, 109 (2013) 220-226.
- [8] K. Thumavichai, Y. Xia, Y. Zhu, Progress in Materials Science, 88 (2017) 281-324.
- [9] M. Farhadian, P. Sangpour, G. Hosseinzadeh, Journal of Energy Chemistry, 24 (2015) 171-177.
- [10] X. Wang, H. Fan, P. Ren, Advanced Powder Technology, 28 (2017) 2549-2555.

- [11] G. Zheng, J. Wang, H. Li, Y. Li, P. Hu, *Applied Catalysis B: Environmental*, 265(2020) 118561.
- [12] S. Beknalkar, V. Patil, N. Harale, M. Suryawanshi, A. Patil, V. Patil, J. Kim, P. Patil, *Sensors and Actuators A: Physical*, 304 (2020) 111882.
- [13] S. Chandrasekaran, E.J. Kim, J.S. Chung, I.-K. Yoo, V. Senthilkumar, Y.S. Kim, C.R. Bowen, V. Adamaki, S.H. Hur, *Chemical Engineering Journal*, 309 (2017) 682-690.
- [14] S. Chandrasekaran, S.H. Hur, W.M. Choi, J.S. Chung, E.J. Kim, *Materials Letters*, 160 (2015) 92-95.
- [15] Y. Qian, M. Yang, F. Zhang, J. Du, K. Li, X. Lin, X. Zhu, Y. Lu, W. Wang, D.J. Kang, *Materials Characterization*, 142 (2018) 43-49.
- [16] L. Xia, J. Bai, J. Li, Q. Zeng, X. Li, B. Zhou, *Applied Catalysis B: Environmental*, 183 (2016) 224-230.
- [17] S. Chen, Y. Hu, S. Meng, X. Fu, *Applied Catalysis B: Environmental*, 150 (2014) 564-573.
- [18] E. Grilla, A. Petala, Z. Frontistis, I.K. Konstantinou, D.I. Kondarides, D. Mantzavinos, *Applied Catalysis B: Environmental*, 231 (2018) 73-81.
- [19] Y. Bu, Z. Chen, C. Sun, *Applied Catalysis B: Environmental*, 179 (2015) 363-371.
- [20] S. Songara, V. Gupta, M.K. Patra, J. Singh, L. Saini, G.S. Gowd, S.R. Vadera, N. Kumar, *Journal of Physics and Chemistry of Solids*, 73 (2012) 851-857.
- [21] M. Takács, C. Dücső, A.E. Pap, *Sensors and Actuators B: Chemical*, 221 (2015) 281-289.
- [22] R. Ponnusamy, A. Gangan, B. Chakraborty, C. Sekhar Rout, *Journal of Applied Physics*, 123 (2018) 024701.
- [23] H. Cho, C. Yun, S. Yoo, *Optics express*, 18 (2010) 3404-3414.
- [24] M. Kang, J. Liang, F. Wang, X. Chen, Y. Lu, J. Zhang, *Materials Research Bulletin*, 121 (2020) 110614.
- [25] L.B. Chandrasekar, R. Chandramohan, R. Vijayalakshmi, S. Chandrasekaran, *International Nano Letters*, 5 (2015) 71-75.
- [26] S. Chandrasekaran, R. Misra, *Materials Technology*, 28 (2013) 228-233.
- [27] S. Aripnammal, S. Chandrasekaran, S. Arumugam, S.E. Muthu, *Digest Journal of Nanomaterials & Biostructures (DJNB)*, 8 (2013).
- [28] X. Xia, Y. Zhang, D. Chao, C. Guan, Y. Zhang, L. Li, X. Ge, I.M. Bacho, J. Tu, H.J. Fan, *Nanoscale*, 6 (2014) 5008-5048.
- [29] Z. Gu, H. Li, T. Zhai, W. Yang, Y. Xia, Y. Ma, J. Yao, *Journal of Solid State Chemistry*, 180 (2007) 98-105.
- [30] X. Li, G. Zhang, F. Cheng, B. Guo, J. Chen, *Journal of the Electrochemical Society*, 153 (2006) H133-H137.
- [31] I.M. Szilágyi, S. Saukko, J. Mizsei, A.L. Tóth, J. Madarász, G. Pokol, *Solid state sciences*, 12 (2010) 1857-1860.
- [32] C.S. Blackman, I.P. Parkin, *Chemistry of materials*, 17 (2005) 1583-1590.
- [33] M. Daniel, B. Desbat, J. Lassegues, B. Gerand, M. Figlarz, *Journal of solid state chemistry*, 67 (1987) 235-247.
- [34] E. Haro-Poniatowski, M. Jouanne, J. Morhange, C. Julien, R. Diamant, M. Fernández-Guasti, G. Fuentes, J. Alonso, *Applied surface science*, 127 (1998) 674-678.